Extensive somatic L1 retrotransposition in colorectal tumors

Szilvia Solyom, Adam D. Ewing, Eric P. Rahrmann, et al.

Genome Res. published online September 11, 2012
Access the most recent version at doi:10.1101/gr.145235.112

Extensive somatic L1 retrotransposition in colorectal tumors

Szilvia Solyom[1†], Adam D. Ewing[2†], Eric P. Rahrmann[3], Tara Doucet[1,9], Heather H. Nelson[4], Michael B. Burns[3], Reuben S. Harris[3], David F. Sigmon[1], Alex Casella[1], Bracha Erlanger[5], Sarah Wheelan[5], Kyle R. Upton[6], Ruchi Shukla[7], Geoffrey J. Faulkner[6,7,8], David A. Largaespada[3], and Haig H. Kazazian, Jr.[1*]

1) McKusick-Nathans Institute of Genetic Medicine, Johns Hopkins University School of Medicine, Baltimore, MD 21205, USA

2) Center for Biomolecular Science and Engineering, University of California at Santa Cruz, Santa Cruz, California 95064, USA

3) Department of Genetics, Cell Biology and Development and Pediatrics, Masonic Cancer Center, University of Minnesota, Minneapolis, Minnesota, USA

4) Division of Epidemiology and Community Health, Masonic Cancer Center, University of Minnesota, Minneapolis, MN 55455, USA

5) Department of Statistics and Oncology, Johns Hopkins University School of Medicine, Baltimore, MD 21205, USA

6) Cancer Biology Program, Mater Medical Research Institute, South Brisbane, Queensland 4101, Australia.

7) Division of Genetics and Genomics, The Roslin Institute and Royal (Dick) School of Veterinary Studies, University of Edinburgh, Easter Bush, EH25 9RG, UK.

8) School of Biomedical Sciences, University of Queensland, Brisbane, Queensland 4072, Australia.

9) Pre-doctoral training program in Human Genetics, McKusick-Nathans Institute of Genetic Medicine, Johns Hopkins University School of Medicine, Baltimore, MD, 21205, USA

† These authors contributed equally to this work and should be considered joint first authors.

* Correspondence to: Haig. H. Kazazian, Jr., Johns Hopkins University School of Medicine, Broadway Research Building, Room 439, 733 N. Broadway, Baltimore, MD 21205, USA. Tel: +1 4105026660; Fax: +1 4105022006; Email: kazazian@jhmi.edu

ABSTRACT

L1 retrotransposons comprise 17% of the human genome, and are its only autonomous mobile elements. Although L1-induced insertional mutagenesis causes Mendelian disease, their mutagenic load in cancer has been elusive. Using L1-targeted re-sequencing of 16 colorectal tumor and matched normal DNAs, we found that certain cancers were excessively mutagenized by human-specific L1s, while no verifiable insertions were present in normal tissues. We confirmed *de novo* L1 insertions in malignancy by both validating and sequencing 69/107 tumor-specific insertions and retrieving both 5' and 3' junctions for 35. In contrast to germline polymorphic L1s, all insertions were severely 5' truncated. Validated insertion numbers varied from up to 17 in some tumors to none in 3 others, and correlated with the age of the patients. Numerous genes with a role in tumorigenesis were targeted, including *ODZ3*, *ROBO2*, *PTPRM*, *PCM1*, and *CDH11*. Thus, somatic retrotransposition may play an etiologic role in colorectal cancer.

INTRODUCTION

Over two-thirds of our genome may stem from “jumping genes” (de Koning et al. 2011). Three classes of retroelements are known to be currently active and a source of human disease: long interspersed elements (LINEs), the prototype of which is the RNA polymerase II transcribed L1, short interspersed elements (SINEs), consisting essentially of RNA polymerase III transcribed Alus, and SVAs (SINE-R/VNTR/Alus) that are intermediate in size relative to Alus and L1s, and are likely transcribed by RNA polymerase II. A fourth class of retroelements in our genome, human endogenous retroviruses (HERVs) is considered immobile. Full-length L1s are not only responsible for mobilizing themselves, but also for mobilizing the non-autonomous Alu (Dewannieux, et al. 2003) and SVA retrotransposons (Ostertag et al. 2003, Raiz et al. 2011, Hancks et al. 2011), inactive L1s (Moran et al. 1996), small RNAs (Gilbert et al. 2005), and classical mRNAs, thereby creating processed pseudogenes (Esnault et al. 2000, Wei et al. 2001; Ohshima et al. 2003).

Although there are about half a million L1s in the human genome, only the human-specific L1s (L1Hs) are currently active, represented in each individual by about 800 germline copies (Ewing and Kazazian 2010), including approximately 200 full-length sequences (Boissinot et al. 2000). According to conservative estimates there are only about 100 active L1Hs in any human diploid genome that are retrotranspositionally competent, of which 6 from the reference genome and 37 from 6 other genomes are known to be highly active (“hot”) (Brouha et al. 2003; Beck et al. 2010). L1s retrotranspose through a process called target primed reverse transcription (TPRT) (Luan et al. 1993; Cost et al. 2002) with the help of the L1-encoded proteins open

reading frame 1 protein (ORF1p) and ORF2p. Endonuclease and reverse transcriptase activities for L1 integration are provided by ORF2p (Mathias et al. 1991; Feng et al. 1996). The hallmarks of TPRT are the addition of a new poly(A) tail to the integrated sequence and target site duplication (TSD), usually 6-20 bp in length. A fraction of retrotransposition events are also associated with 3' transduction, the co-mobilization of 3' flanking DNA sequences (Holmes et al. 1994; Moran et al. 1999; Goodier et al. 2000; Pickeral et al. 2000), resulting from transcriptional read-through of the weak L1 poly(A) signal and preferential use of a stronger downstream poly(A) signal. Most *de novo* L1 retrotransposition events are 5' truncated (Gilbert et al. 2005), with one extreme truncation described where the whole L1 sequence was missing and only the 3' transduced sequence was present (Solyom et al. 2012).

Active mobile elements are not only a significant source of intra- and inter-individual variation, but can also act as insertional mutagens. There are 97 known disease-associated retrotransposon insertions into protein coding genes (Hancks and Kazazian, 2012; van der Klift et al. 2012), which is an underestimate as conventional mutation screening methods are not designed to amplify large insertions. Of these nearly 100 cases, 25 are caused by L1s, 60 by Alus, 8 by SVAs, and 4 by poly(A) sequence originating from an unidentifiable source (Hancks and Kazazian, 2012; van der Klift et al. 2012). Of these insertions, 30 occur in cancer cases, including 4 in colon cancer patients (Miki et al. 1992; Su et al. 2000; Kloor et al. 2004; van der Klift et al. 2012). While 3 of the 4 colon cancer cases involve predicted germline or early somatic insertions, a somatic L1 insertion occurred in the *APC* gene in colon cancer (Miki et al. 1992).

In addition to acting as insertional mutagens, retrotransposons can disrupt gene function and genomic integrity in many other ways. These include recombination-mediated gene rearrangements, genetic instability, transcriptional interference, alternative splicing, gene breaking, epigenetic effects, the generation of DNA double-strand breaks, and the expression of small non-coding RNAs (reviewed by Goodier and Kazazian, 2008; Beck et al. 2011). All these mechanisms are compatible with a tumorigenic potential of these elements. Retrotransposon overdose is another potential scenario in malignancy and could result in increased insertional mutagenesis, toxicity or other oncogenic effects. Indeed, the over-expression of L1 ORF1p was observed in certain tumors (Bratthauer and Fanning, 1992; Asch et al. 1996; Su et al. 2007; Harris et al. 2010), and RNAi-mediated silencing of L1s resulted in reduced proliferation and differentiation of tumorigenic cell lines (Oricchio et al. 2007). In addition, overexpression of Alu elements may exert disease through RNA toxicity (Kaneko et al. 2011). Thus, the cell likely has intrinsic defense mechanisms to prevent retrotransposon overexpression, including methylation (Yoder et al. 1997, Bourc'his and Bestor, 2004) and the expression of several host proteins, such as APOBEC3 family members (Chen et al. 2006, Bogerd et al. 2006; Muckenfuss et al. 2006, Stenglein et al. 2006) or DNA repair enzymes (Gasior et al. 2006, Suzuki et al. 2009; Coufal et al. 2011).

Here we applied two high-throughput L1-targeted re-sequencing methods to discover retrotransposon activity in colorectal cancers. We identified numerous non-reference L1 insertions not present in paired normal tissue and report a high retrotransposon insertion rate in tumors. We characterized insertion size and TSDs in

cancer tissue, confirming that L1s primarily mobilize in cancer via TPRT. The data suggest the importance of retrotransposition in the biology of colorectal tumorigenesis.

RESULTS

L1 display through high-throughput sequencing

We applied two next generation re-sequencing methods – hemi-specific PCR coupled to Illumina sequencing (L1-seq) (Ewing and Kazazian, 2010) and retrotransposon capture sequencing (RC-seq) (Baillie et al. 2011) to interrogate the retroelement load of colorectal tumors. Approximately 800 non-reference L1Hs copies had been located from individual blood or lymphoblastoid cell lines by L1-seq – the same number as represented by the hg18 reference genome assembly, indicating its capacity to recover essentially all germline L1Hs elements (Ewing and Kazazian, 2010). Here, we applied this method to recover somatic insertions from malignant tissues. RC-seq has previously been used to identify somatic mosaicism associated with L1, Alu and SVA mobilization in the brain (Baillie et al. 2011). Its use of sequence capture for retrotransposon enrichment contrasts with the use of PCR by L1-seq; as a result RC-seq is expected to cover a broader range of insertions, but with less depth per insertion than L1-seq. A highly multiplexed version of RC-seq was applied to assess whether somatic L1Hs insertions were identified by both approaches.

We sequenced DNA from 16 colorectal tumors and matched normal colons using a pooled L1-seq-based approach. The 16 tumor/normal pairs (32 samples total) were separated into 4 libraries of 8 samples each denoted ‘colo1/tumor’, ‘colo1/normal’, ‘colo2/tumor’, and ‘colo2/normal’. We sequenced one lane for each library on an Illumina HiSeq 2000 instrument with the exception of colo1/normal, where two lanes of data were generated. The total number of reads generated for each library can be found in Table S1.

Using computational methods outlined in Ewing and Kazazian (2010), we identified clusters of reads localized 3' of predicted insertion sites. We required 100 reads spanning at least 100 bp ('high stringency') as a minimum for L1 detection, which yields a specificity of greater than 90% based on recovery of reference L1 insertions and non-reference sites discovered in previous studies (see Fig. S1 and S2 for an exploration of cutoff parameters). Using these criteria, we identified 764 reference L1Hs insertion sites present in NCBI36/hg18 and 400 non-reference insertion sites from the colo1 data. From the colo2 data we identified 816 reference and 433 non-reference insertions. Combining the data, we found 819 reference L1Hs elements and 635 non-reference elements, 336 of which had not been previously cataloged. Many of these uncataloged elements are new somatic insertions in the tumor. In total, 38% of reference and 35% of non-reference insertions were in gene annotations based on UCSC Known Genes. The distribution of L1 insertions detected by L1-seq in this study is shown in Figure 1.

Our primary interest in generating these data was in finding insertions present either in a cancer pooled library or in a normal pooled library, and not present in the corresponding paired normal or tumor library. Turning to these, with the same stringency cutoffs as above, we found 35 putative insertions only in colo1/tumor, 4 only in colo1/normal, 50 predictions only in colo2/tumor, and 8 only in colo2/normal. Decreasing the requirements for predicted insertions to 10 reads spanning at least 100 bp ('low stringency'), we found 69 potential insertions only in colo1/tumor, 173 only in colo1/normal, 75 only in colo2/tumor and 42 only in colo2/normal. The dramatic increase in predictions for colo1/normal only with decreasing stringency is an effect of

the higher coverage in the colo1/normal versus colo1/tumor (Table S1), as two lanes of sequence were generated for colo1/normal.

Five of the L1-sequenced colorectal tissue pairs were barcoded, pooled, and analyzed by shallow, multiplexed RC-seq (10 libraries, ~75 million paired-end GAIIx reads). A total of 26,903 non-reference genomic insertions were detected by at least one read (Table S2). Of these, 358 were a) found in only one donor b) were not identified in RC-seq previously performed on pooled blood (Baillie et al. 2011) or databases of retrotransposon polymorphisms (Ewing and Kazazian, 2011, Iskow et al. 2010, Huang et al. 2010) and c) could be annotated with high confidence due to detection by multiple unique amplicons. Of this set, 96 were only found in tumor, including 8 L1, 83 Alu and 5 SVA. 39 insertions were found only in non-tumor sample and 223 were found in both tumor and non-tumor. The tumor:non-tumor ratios for L1, Alu and SVA were approximately 8:1, 2.5:1 and 2:1, respectively. AluY and L1-Ta/pre-Ta were detected, but no HERVs were detected.

PCR validation

We applied a step-wise PCR amplification scheme to validate insertion sites from L1-seq data and to determine both 5' and 3' junctions of L1Hs elements identified by L1-seq. Primary validations focused on confirming the presence of *de novo* L1 inserts by amplifying their 3' junction and determining which of the 8 patients carried the insertion within a DNA pool (PCR scheme and primer design performed according to Ewing and Kazazian, 2010, Fig. 2A and Fig. 2B). An L1 insertion was considered to be validated as tumor-specific if the filled site (L1-containing) PCR product was present in the tumor, but

not in the paired normal tissue, and in case of heterozygous autosomal insertions, the empty site PCR product (WT allele) was amplified from both members of the tissue pair. Using a single PCR condition to amplify the 3' junctions, we PCR-validated 26/40 and 37/51 insertions from the colo1 and colo2 high stringency data sets, respectively. We also set out to PCR amplify 16 colo1 insertions represented by less than 100 Illumina reads and were able to validate 9. Thus, we PCR-validated before sequencing the 3' ends of 72 of 107 putative insertions (Table S3, Text S1).

Interestingly, among 12 high stringency putative insertions from normal colon of the combined colo1 and colo2 data sets, none could be validated. Possible explanations for false positives in the L1-seq data include PCR artifacts arising during library preparation, suboptimal PCR conditions used for validation, or L1 insertion into repetitive sequences, refractory to successful primer design.

Our step-wise PCR amplification scheme continued by retrieving the 5' junctions of tumor-specific L1 insertion events. Several empty site PCRs had already yielded a higher molecular weight band exclusively in the tumor, which in each case was verified to be a highly truncated L1 element (Fig. 2B). In the remaining cases, long-range PCR and a PCR specifically designed to amplify the 5' end of a full-length L1 were employed to retrieve the 5' junction.

Altogether, out of 72 cases where the insertions were PCR-validated to be tumor-specific, we successfully sequenced either the 3' or the 5' junction in 69 cases (Table S3, Text S1). For 35 insertions, we sequenced both junctions, enabling us to characterize TSDs and L1 insertion size in cancer tissue (Table 1). Surprisingly, all of

the tumor-specific insertions were highly truncated, the mean L1 insertion size being 585 bp excluding the poly(A) tail (Table 1).

Using a PCR designed to amplify full-length L1 insertions, we failed to amplify the 5' end of any of the remaining tumor-specific insertions where 5' junctions could not be identified with the previous PCR approaches. On the other hand, 3 of 10 germline polymorphic insertions had an intact 5' end, in agreement with 30% of reference L1Hs elements being full length (Pavlicek et al. 2002). This difference between full length L1 insertions in tumors (~0%) versus full length insertions among polymorphic germline L1Hs (~30%) is statistically significant (p=0.016, Fisher's exact test), and is a clear departure from what is observed from the reference genome and from heritable non-reference insertions (Ewing and Kazazian, 2010).

L1-seq results on 5 tumors were corroborated by RC-seq. Eleven high confidence L1Hs hits were found in these cancers by L1-seq, out of which four were also detected by RC-seq at either the 5' or 3' junction (ins. 5, 9, 14, and 32) (Table S2, Table S3, Text S1). Among 8 high confidence L1 insertions within genes detected by RC-seq, but missed by L1-seq, one was validated as present in tumor 10, targeting the *DGKI* gene (Table S2, Figure 3). Of the remaining putative tumor-specific insertions that could be PCR-amplified, 6 of 8 L1s, 30 of 57 Alus, and 6 of 11 SVAs were present in both tumor and paired normal tissue. No other confirmed tumor-specific insertions from the L1-seq data were found by RC-seq.

In order to determine if L1s are frequently mobilized in other non-malignant somatic tissues, we performed L1-seq on genomic DNA extracted from cerebrum, liver, and testis samples from two other individuals (cadaver samples) who had died from

arteriosclerotic cardiovascular disease. None of the Illumina high-stringency sequence peaks suggestive of somatic L1 insertion could be PCR-validated, implying that the high rate of somatic L1 insertions observed in colon cancer was specific to the malignant tissue. Thus, we have no evidence from our data of somatic insertions in normal colon, liver, testis, or cerebrum.

Characterization of tumor-specific insertions

Intriguingly, the number of validated L1 insertions varied widely from tumor to tumor with up to 17 insertions in some and none in 3 others (Figure 3). Most retrotransposition events showed hallmarks of TPRT, namely TSD (27/35), L1 endonuclease cleavage site, the presence of L1 poly(A) tail, frequent 5' inversion (10/35), and in one case, a 3' transduction (Table 1). However, we note that a substantial fraction of these somatic insertions (8/35) lacked a TSD and 6 of these lacked a discernible endonuclease cleavage site, suggesting that they were endonuclease-independent insertions (Morrish et al. 2001). Two insertions ("3" and "21") contained 3' sequence from other chromosomes, but lacked a poly(A) tail in between the two sequences that would indicate a 3' transduction. Thus, they are likely cancer-associated recombination events (Table S3, Text S1).

Numerous genes were targets for insertional mutagenesis in colon tumors by L1s that are represented in the COSMIC database (Catalogue of Somatic Mutations in Cancer, http://www.sanger.ac.uk/genetics/CGP/cosmic/). Examples include *PTPRM* (protein tyrosine phosphatase, receptor type, M), *ODZ3* (odd Oz/ten-m homolog 3), *ROBO2* (roundabout, axon guidance receptor, homolog 2), *PCM1* (pericentriolar

material 1), and *CDH11* (cadherin-11). *PCM1* and *CDH11* are also represented in Sanger's Cancer Gene Census (http://www.sanger.ac.uk/genetics/CGP/Census/). Interestingly, according to COSMIC, in the large intestine these genes were mutated with the following high frequencies: *PTPRM* (50%), *ODZ3* (100%), *ROBO2* (15%), *PCM1* (12%), *CDH11* (52%). All of our hits were intronic, and were PCR validated as well as sequenced. Additional interesting genes with a potential role in malignancy were also targeted, for instance *RUNX1T1* (runt-related transcription factor 1), a member of the myeloid translocation genes. Interestingly, somatic *RUNX1T1* point mutations were not only found in colorectal cancers (Wood et al. 2007), but the product of the related *RUNX3* gene regulates L1 expression (Yang et al. 2003).

Cellular timing of L1 retrotransposition

In an effort to determine at what point in tumorigenesis the L1 insertions occurred, we developed three lines of evidence: analysis of SNPs in sequence flanking the L1 insertion and the empty site, the number of empty site X chromosome alleles in males who had an L1 insertion into the X, and the presence/absence of the L1 insertion in a second section of a particular tumor in which an L1 insertion occurred.

First, we found three insertions (C2, C4, and insertion 31) with flanking heterozygous SNPs. For C2 (*ODZ3* gene) there was 1 SNP, for C4 there were 4 SNPs, and for insertion 31 there was 1 flanking SNP (Fig. S3A). The presence of both alleles of the particular SNP in the empty site chromosomes is informative in case of no aneuploidy at the respective alleles. If the insertion occurred at the initiation of the tumor (the one-cell stage), the filled site would contain one allele and the empty site would

contain the other allele only. If both alleles are present in the empty site chromosomes, then the insertion likely occurred after the one-cell stage of the tumor. The data showed that all 6 SNPs near 3 different insertions in the empty site chromosomes were heterozygous, suggesting that the insertions occurred after the initiation of tumorigenesis. We carried out array comparative genomic hybridization (aCGH) and found no copy number gain or loss in the chromosomal arm of these SNPs (data not shown), although small chromosomal aberrations at the respective alleles can not be ruled out.

Second, we found insertions (D9, D12, and E3) into the X chromosome in two males. If the insertion occurred at the one cell stage and the male did not have X-chromosome aneuploidy, the tumor should lack an empty site. However, in all cases, we found an empty site band by PCR, indicating again that the insertions occurred after the one-cell stage of tumorigenesis (Fig. S3B contains data on D9 and D12). Again, aCGH showed that both males had a single X chromosome.

Third, we obtained a second portion of tissue from a number of tumors and determined whether the insertions found in the first tumor tissues could be confirmed in the second tumor sample. In 3 of 7 instances (insertions C2, D7, and E3) we were able to confirm the insertion in a second tumor sample, suggesting a relatively early event in tumorigenesis. Four other insertions (“31”, “A10”, “C4”, “D12”) were present in the first tumor section, but not in the second (Fig. S3C). In tumor 2853, 2 insertions were studied: E3 was present in both tumor portions, while D12 was not, suggesting that these two insertions occurred at different times and in different cells of the tumor (data not shown). Furthermore, heterozygosity for L1 flanking SNPs in insertions 31 and C4 in

the original tumor sample, as well as the absence of the insertion from the second tumor portion both suggest late insertion events. Thus, from the combination of these data on a small sample size we conclude that most, if not all, of the studied L1 insertions occurred after the initiation of the tumor. However, a minority of the insertions may have occurred at an early stage of tumorigenesis. Furthermore, we cannot exclude the possibility of tumor blood vessels or infiltrating lymphocytes as contributing alternative explanations for some of the results.

Effects of L1 retrotransposition on measures of cellular instability

To address the increased rate of somatic L1 retrotransposition in tumors, we assessed the genomic landscape of the tissue samples by aCGH, microsatellite instability (MSI), and L1 promoter methylation status. A previous report demonstrated a correlation of genome-wide DNA methylation status of tumors with increased *de novo* L1 insertions (Iskow et al. 2010). We assessed the methylation status of the L1 promoter at 4 different CpG sites. Although L1 promoter hypomethylation was found in tumor samples compared to paired normal tissue, no correlation was observed between L1 methylation status and the number of L1 insertions (Fig. 4A).

For aCGH, we analyzed normal and tumor tissue from 6 patient samples, two that possessed the greatest number of *de novo* tumor insertions (12 and 1775), two with no tumor insertions (8 and 7647), and the two males mentioned above with both empty and filled insertion sites in X chromosomes (17 and 2853). Tumor samples 8, 12, 17, and 1775 contained complex chromosomal changes, including entire and partial chromosomal gains and losses. Tumor samples 2853 and 7647 presented no

detectable aberrations relative to normal tissue. Interestingly, 3 of the samples (12, 17, and 1775) with complex chromosomal rearrangements had a high number of validated insertions. Likewise, patient 7647 with no validated L1 insertions had no detectable chromosomal changes. The outliers from the trend of a direct relationship between chromosomal aberrations and L1 insertions were patients 8 and 2853. Interestingly, these latter patients are potentially genetically predisposed to colon cancer due to familial cancer aggregation or very young age of diagnosis.

In addition to analysis of gross genomic abnormalities, we assessed the status of the mismatch DNA repair pathway by assessing microsatellite expansions in the genome. Seven of the 16 patients were MSI positive. Although two samples with the highest number of somatic L1 insertions were MSI positive, MSI status did not correlate with the number of *de novo* L1 insertions for each tumor (Fig. 4B).

Interestingly, a statistically significant correlation was observed between the number of insertions and the age of the investigated patients ($p=0.01425$, $R^2= 0.3128$, where age is the time of surgical sample removal). Eight or more validated insertions were observed only in the tumors of patients 78 years old or older. An outlier in the correlation was a 72-year-old with no validated insertions. However, he was the only proband with rectal cancer, but no colon tumor diagnosis. When this patient was excluded from the analysis, as well as cases with a presumed genetic predisposition to colon cancer (familial polyposis case and a 17-year-old male), an even more significant correlation was observed between the age of sporadic colon cancer patients and L1 activity ($p=0.001548$, $R^2= 0.578$, Fig. 4C).

DISCUSSION

Our L1-seq method has revealed a high rate of L1Hs retrotransposition in certain colorectal cancer genomes. The neighboring matched normal colon sample in these 16 cases, as well as cerebrum, liver, and testis from two other individuals yielded no L1 insertions that could be validated, indicating few or no retrotransposition events in these normal tissues.

Iskow et al. (2010) used 454 pyrosequencing to search for *de novo* L1 insertions in five glioblastomas, five medulloblastomas, as well as leukemia and breast cancer cell lines, but they found no insertions in these cases. However, they identified 9 somatic L1 insertions in 6 of 20 lung tumors. Since TSDs were not reported, the question of whether L1 integration in lung cancer occurs through TPRT remained open.

Here we report that evolutionarily young L1Hs retrotransposons can mobilize themselves through the classical TPRT mechanism in colon cancer genomes at a high frequency. The true retrotransposition rate is likely to be even higher, as our method does not detect insertions mobilized by L1 elements in trans, such as Alus, SVAs, most inactive L1s, and processed pseudogenes. In addition, there are likely other L1 insertions in our dataset that have not been subjected to validation. Longer tumor-specific 3' transductions will be missed as well, as it is difficult to differentiate between the progenitor and the transduced sequence by their 3' flank with L1-seq.

In order to determine why the rate of somatic cell retrotransposition was high in some tumors compared to the normal tissue, we assessed how the following factors correlate with retrotransposition rate: age of colorectal cancer patients, chromosomal aberrations, L1 methylation status, and mismatch DNA repair as reflected by MSI. A

clear correlation of retrotransposition activity was observed with the age of colon cancer patients in sporadic cases. Furthermore, we also analyzed genetic instability by aCGH in 6 samples and found a modest association between the number of chromosomal aberrations and the age of the sporadic colon cancer patients. Altogether, it is possible that the hypomethylated microenvironment of the tumors, together with genetic instability as reflected by MSI and gross chromosomal changes, have a cumulative effect in older patients. Our results are in agreement with the correlation of retrotransposition activity with genome instability during yeast chronological aging (Maxwell et al. 2011).

In this study, we found that genes with a known driver function in cancer are mutagenized by L1Hs elements. The accumulation of retrotransposon sequences is predicted to cause further genetic instability through recombination. Thus, an elevated insertion rate is expected to contribute to tumor evolution. As exemplified by a somatic L1 insertion into the *APC* gene (Miki et al. 1992), it is clear that in some fraction of colorectal cancers retrotransposon insertions can be etiologically significant. Yet it remains unclear in what fraction of cases retrotransposons initiate malignant transformation and in how many instances they contribute solely to a more aggressive phenotype. SNP, X chromosome, and secondary sampling data from tumor samples suggest that L1 insertions likely occurred at various times after the initiation of the tumor. Although we found no evidence for L1 insertion into colon cancer tumor suppressor genes or oncogenes that would be indicative of driver mutation-induced tumor clonality, analysis of a larger number of tumors or a deeper sequencing of retrotransposon insertions could uncover such events. We propose that it is possible to

estimate insertion timing and tumor heterogeneity more precisely by evaluating pure tumor samples. Our findings are in agreement with a very recent report on retrotransposon insertions in epithelial cancers (Lee et al. 2012). Intriguingly, an intronic L1 integration event was found in that study as well into the *ROBO2* gene in a colon tumor. Additionally, they detected intronic L1 insertions in *CDH12*, while we characterized an insertion into the *CDH11* gene. Thus, the role of cell adhesion genes in retrotransposon insertion-mediated colorectal tumorigenesis may deserve further investigation.

An unexpected finding of our PCR-based validation is the severely truncated nature of all validated L1 insertions in colon cancer. It was not possible to assess whether this is a general characteristic of the malignant phenotype, of all somatic tissues, or of the gastrointestinal tract, in particular, as no *de novo* L1 insertions could be uncovered from normal colon, liver, testis, and brain. In a transgenic mouse model, 30 of 33 somatic L1 insertions were 5' truncated (Babushok et al. 2006), raising the possibility of a gradual decrease in L1 size from germline to somatic to malignant insertions. In cultured HeLa cells, 94/100 insertions were 5' truncated (Gilbert et al. 2005). This might indicate that some cancer tissues or cultured cells could allow full length insertions to accumulate. The overexpression of an exogenous L1 element, coupled with the bias towards recovering larger inserts in that assay, and the unknown effects of cell culture conditions on retrotransposition complicate transferring conclusions on L1 5' truncation rate to cancer tissue. Likewise, it is not understood why the majority of germline L1 insertions are 5' truncated as opposed to Alu and SVA insertions that are mostly full length, yet also mobilized by L1s (Hancks et al. 2011).

The truncated structure of L1 elements in colorectal cancer may be useful in understanding the mechanism of 5' truncation both in normal and tumor cells. We propose two possible explanations: (1) if TPRT timing is coupled to the cell cycle, the elevated cell division rate of malignant cells may not leave sufficient time to complete integration of long mobile elements; (2) a DNA repair pathway might monitor and remove *de novo* mobile element insertions in healthy tissues. Once this presumed surveillance pathway is down-regulated in cancer, retrotransposon insertions are not removed efficiently and allowed to accumulate. At the same time, another or the same DNA repair pathway might specialize in truncating fresh integrants or prohibiting them from completing retrotransposition. If this process is upregulated, the truncation rate increases. The efficiency of such a pathway might correlate with insertion size or be sequence specific, thus preferentially targeting L1 elements over Alus and SVAs. Interestingly, non-homologous end joining (NHEJ) is an important DNA repair pathway candidate with a reported conflicting dual role in regulating retrotransposon insertions, offering an explanation for parallel L1 upregulation and truncation (Suzuki et al. 2009). We propose that by comparing the genome or transcriptome of tumors with a high rate of retrotransposition to their paired normal tissues, we may discern clues to cellular factors causing L1 mobilization and 5' truncation.

To conclude, the cancerous colon of many patients is the second reported organ besides the brain (Baillie et al. 2011) in which a high rate of retrotransposition occurs. Lung, prostate and ovarian tumors are also reported to allow a lower level of L1 mobilization (Iskow et al. 2010; Lee et al. 2012), but many other cancer types appear to be non-permissive for a detectable rate of retrotransposition. All L1 insertions in the

colorectal tumors of this study were highly truncated, potentially indicating the footprint of a defective or hyperactive DNA repair pathway in cancer. The cause and effect of retrotransposon mobilization in cancers warrants further investigation.

METHODS

Human DNA samples

DNA was extracted from human patient tissue samples acquired from the University of Minnesota Tissue Procurement Facility from BioNet (IRB#0805E32181). See Table S4 for patient data. Briefly, 2 mg of tissue was digested overnight at 55ºC on a rotating platform in 710 µl of digest buffer (1 M TRIS pH=8.0, 1 mM EDTA, 1X SSC, 1% SDS, 1 Mm NaCl, 10 µg/ml Proteinase K. Following digest, DNA was purified using phenol-chloroform-isoamyl alcohol (Life Sciences) isolation protocol.

Human frozen tissues from two Caucasian cadavers with arteriosclerotic cardiovascular disease were obtained from the NICHD Brain and Tissue Bank for Developmental Disorders at the University of Maryland, Baltimore. DNA isolation was done utilizing the AllPrep DNA/RNA Mini Kit (Qiagen).

Library construction, sequencing and analysis

L1-seq

The library for L1Hs elements was made according to Ewing and Kazazian (2010), while the library for L1, Alu, and SVA elements (RC-seq) was constructed

according to Baillie et al. (2011). L1Hs elements were TOPO-TA cloned (Invitrogen) and Sanger-sequenced for quality control of the library preparation, and were subsequently sequenced on an Illumina HiSeq 2000 at the Johns Hopkins University Genetic Resources Core Facility High Throughput Sequencing Center.

Pooled L1-seq library sequence data was analyzed as described previously (Ewing and Kazazian, 2010), and compared against insertion sites of known reference and non-reference transposable elements (Huang et al. 2010 Beck et al. 2010; Ewing and Kazazian, 2010; Hormozdiari et al. 2011; Iskow et al. 2010; Witherspoon et al. 2010; Ewing and Kazazian, 2011; Stewart et al. 2011). Gene annotations were obtained from UCSC Known Genes (Hsu et al. 2006).

RC-seq

The library for retrotransposon capture and sequencing was created utilizing DNA from 5 pairs of colorectal and normal tissue (samples 1; 4; 6; 8; 10) by the same method as published previously (Baillie et al. 2011). One significant change was made to the technique, in that liquid phase hybridization was performed as opposed to solid surface, chip-based hybridization. The libraries were then sequenced on an Illumina Genome Analyzer II and aligned to the genome by a computational pipeline that utilized SOAP2 to align reads to the genome and employed much the same method as published (Ballie et al. 2011, Shukla et al. 2012: under review).

PCR validation of the Illumina results

A 3-step PCR validation protocol was used to validate the next generation sequencing reads and to retrieve 3' and 5' junctions. As the first step, L1 3′ ends together with flanking genomic regions were amplified using the same AC dinucleotide–specific primer of L1Hs as used for Illumina sequencing (L1Hs primer: GGGAGATATACCTAATGCTAGATGACAC) and a primer selected from the 3′ flanking region based on the reference genome sequence (FS primer). PCR reactions were carried out in 12.5 µl 2x GoTaq Green master mix (Promega) in a total volume of 25 µl, with 0.8 µl of FS primer, 1.5 µl of L1Hs primer, and 25 ng DNA to amplify the filled site. The empty site was amplified with the same conditions, except that 1.5 µl of FS primer, 1.5 µl of ES primer, and 12.5 ng DNA were used. Primers were 20 pmol/µl and their location is depicted in Fig. 2A. Reactions were incubated for 2 min at 95°C followed by 30 cycles of 30 sec at 95°C, 30 sec at 57°C, and 1.5 min at 72°C, followed by final extension of 5 min at 72°C on a PTC-200 Peltier Thermal Cycler. Long-range PCR to recover longer L1 insertions was performed with Expand Long Template PCR System (Roche) according to the manufacturer's instructions in buffer 1, with 1 µl of 20 µM FS and ES primers each, and 25 ng tumor DNA. 5' junctions were PCR amplified using the same conditions as for the 3' junction, except that a primer hybridizing to the L1 5'UTR was used (L1nt112out: GATGAACCCGGTACCTCAGA) together with the respective ES primer, and primer extension time was only 45 s. FS and ES primer sequences are included in the supplemental material (Table S1). PCR products were cut out of the gel, extracted with QIAquick Gel Extraction Kit (Qiagen) and sequenced. See Text S1 for Sanger sequence data on insertions.

Microsatellite Instability assays

To assess the MSI status, we utilized five markers recommended by the National Cancer Institute (Bethesda markers): BAT25 and BAT26 to assess mononucleotide repeats (A)n and D2S123, D5S346, and D17S250 to assess dinucleotide repeats (CA)n. MSI status was determined using previously established protocols (Ashktorab et al. 2003; Muller et al. 2004). Primers were developed by the NCI for screening patients in the clinic.

L1 methylation status

The methylation level of L1 promoters was performed according to Wilhelm et al. (2010). Briefly, each sample was amplified 3 times and each amplification was pyrosequenced once. The average of the three was utilized to determine the value of CpG methylation for each of the 4 positions analyzed for an L1.

aCGH

DNA from patients 8, 12, 17, 1775, 2853, and 7647 were restriction digested and labeled with fluorochrome Cyanine-5 using random primers and exo-Klenow fragment DNA polymerase. DNA from a sex-matched control was labeled concurrently with Cyanine-3. The sample and control DNA were combined and array-based comparative genomic hybridization (aCGH) and single nucleotide polymorphism analysis (SNP) was performed with a 180K Cancer CGH+SNP microarray constructed by Agilent Technologies, Inc that contains approximately 115,000 distinct biological oligonucleotides and 55,000 SNP sites, spaced at an average interval of 25 KB (for

20,000 cancer associated CGH probes: 1 probe/0.5-1 KB). The ratio of sample to control DNA for each oligo was calculated using Feature Extraction software 10.10 (Agilent Technologies). The abnormal threshold was applied using Cytogenomics 2.060 (Agilent Technologies). A combination of several statistical algorithms was applied. A minimum of 3 oligos that have a minimum absolute ratio value of 0.1 (based on a log(2) ratio) is required for reporting of a copy number loss or gain. Analysis was performed using Human Genome Build 19 (Feb 2009) as the reference.

DATA ACCESS

The data are presented in the Supplementary Tables and Files. Any further data is available upon request. The dbGAP accession number assigned to this study is phs000536.v1.p1.

ACKNOWLEDGEMENTS

We thank Ricardo Linares, John L. Goodier, and Prabhat K. Mandal for their great insights into the project and for their comments on the manuscript. We thank David Haussler for advice. Ling Cheung is acknowledged for excellent technical assistance. The cytogenetic analyses were performed in the Cytogenetics Core Laboratory at the University of Minnesota with support from the comprehensive Masonic Cancer Center NIH Grant #P30 CA077598-09. Research in the Kazazian laboratory is funded by grants from the National Institutes of Health awarded to H.H.K. Human tissue was obtained from the NICHD Brain and Tissue Bank for Developmental Disorders at the University of Maryland, Baltimore, MD (NICHD Contract no. N01-HD-4-3368 and NO1-HD-4-3383).

The role of the NICHD Brain and Tissue Bank is to distribute tissue, and therefore, cannot endorse the studies performed or the interpretation of results.

FIGURE LEGENDS

Figure 1: Genomic distribution of L1 insertions.

Outer rings show the density of detected insertion sites for reference (grey) and non-reference (black) L1s. The approximate locations of the 72 PCR-validated somatic insertions are indicated by dots inside the circle. Note, that 69 of the 72 insertions were successfully sequenced.

Figure 2: PCR validation scheme of L1-seq results

Fig. 2A. The 3-step PCR validation scheme and location of primers used. Triangles symbolize TSD.

Fig. 2B. PCR validation of the 3' junction (ins. 7). This insertion is in tumor 1 of the 8 DNA samples that had been pooled for Illumina sequence analysis (left panel), while the right panel shows it is present exclusively in the tumor, but not in the normal colon. The higher molecular weight band visible above ins. 7 empty site PCR product in the tumor is a highly truncated L1. Abbreviations: T, tumor; N, normal colon; FS, filled site PCR product; ES, empty site PCR product.

Figure 3: Distribution of somatic L1 insertions in tumors

Insertions in black were detected by L1-seq, while the insertion in tumor 10 in white was detected by RC-seq only.

Figure 4: Analysis of factors influencing L1 activity. A) L1 CpG promoter methylation status performed by quantitative bisulfite PCR analysis. Abbreviations: N=normal tissue, T=tumor tissue, *=MSI. Replicates of 4 were done for each data point. Error bars represent standard deviations. B) MSI analysis. 6% TBE gel depicting the status of 5 microsatellite repeats (*BAT25*, *BAT26*, *D2S123*, *D17S250*, *D17346* in descending order) in normal and tumor tissue from two different patients. Tumor tissue "6" contained additional bands and gel shifts compared to the normal tissue, indicating MSI. Samples from "8" demonstrated no differences suggestive of MSI. C) Correlation of L1 activity with age of surgical sample removal of the patients. See text for details.

TABLE LEGEND

Table 1: L1Hs insertions in cancer with both 5' and 3' junctions characterized

The L1 5' junction nucleotide position extends until the point where the sequence chromatogram was readable. Inferred L1 size is calculated by hypothesizing that no further L1 deletions occurred. Poly(A) length cannot be determined unambiguously by Sanger sequencing due to different level of polymerase slippage from the forward and reverse sequencing directions. Ins. 5–57 are colo1, and ins. A2-E1 are colo2 L1s.

SUPPLEMENTARY FILES

Figures S1 and S2: Effect of peak size cutoffs on validation rate and number of insertions called for colon tumor/normal paired sample pool 1 (Fig. S1) or pool 2 (Fig. S2).

A) Peak width and number of reads per peak (read count) versus number of known insertions meeting the corresponding cutoffs. In this case, “known insertions” refers to either insertions present in the reference genome assembly or those not present in the reference but presented in one or more studies. The green dot indicates the position of the low stringency cutoff (10 reads per peak, 100 bp width) and blue dot indicates the position of the high stringency cutoff (100 reads per peak, 100 bp width) on the surface. B) Peak width and read count cutoffs versus verification rate where verification rate is defined as the number of peaks corresponding to a known insertion site (reference or non-reference) at a given cutoff divided by the total number of peaks at the same cutoff. The green and blue dots are as indicated in (A).

Figure S3: L1 insertions likely occur after tumor initiation

A) SNP data showing heterozygosity in empty site alleles. Insertions 31, C2, and C4 are present in tumors 12, 2853, and 6645, respectively. Insertion numbers and SNP locations are noted above the chromatograms. Filled sites are shown from the original tumor section. Empty sites are shown from the original and a second tumor section, as well as from the paired normal colon. Note that only insertion C2 was present in the second tumor section, while insertions 31 and C4 were not. B) Insertions into the X chromosome of males still have empty sites, suggesting that they occur after the one-cell stage in the tumors. Insertion D9 occurred in tumor 17, while insertion D12 occurred

in tumor 2853. Insertion E3 in tumor 2853 is not shown. C) Some insertions are present in a second section of the tumor, while others are absent. Insertions C2, D7, and E3 were present in two different portions of the same tumor, suggesting a relatively early event in tumorigenesis. Insertions 31, A10, C4, and D12 were present only in the first tumor section. Representative examples are shown. Abbreviations: F, filled site PCR; E, empty site PCR; TA, alternate section of the tumor sample. Filled site PCR bands are denoted by an arrow.

Table S1 A and B: L1 seq data.

Data on colo1 (Table A) and colo2 (Table B) tumor, normal, and germline (colon-specific) insertions. In Table A 'Polymorphic insertions' sheet lists 10 germline insertions that were used as controls (see Table S3). Columns are locations (chr. as well as hg18 and hg19 genomic coordinates), strand orientation, height (the number of reads in the peak), width (the position of the last base in the peak minus the position of the first), starts (the number of unique alignment positions in the peak), L1 family, pooled sample name, height and width of the peak from the second pool in the preceeding column (zero if the insertion only occurred in one pool), overlapping repeats, whether the L1 is present in another study, gene overlaps, exon overlaps (within 500 bp), and primer sequences. In some cases, alternative primers were used, whose sequences are available upon request. Selecting high stringency insertions (>= 100 bp width, >= 100 Height, family = L1Hs or noL1), there are 764 reference L1Hs insertion sites present in NCBI36/hg18 and 400 non-reference insertion sites (1164 altogether) in the colo1 data

set. Likewise, 1249 high stringency insertions are found in the colo2 data set (816 reference and 433 non-reference ones).

Table S2: RC-seq data.

Sheet 1: RC-seq data from 5 tumor samples are presented and include L1, Alu, and SVA putative insertions. Four of these L1 insertions were detected by L1-seq (highlighted in yellow).

Sheet 2: High stringency RC-seq data showing putative insertions into genes. The L1 insertion into the *DGK1* gene was validated to be tumor-specific (in bold).

Table S3: Results of the 3-step PCR validation process

This table summarizes the results of the PCR validation steps. Columns are insertion code, chr. location in hg18 and 19, tumor sample that contained the insertion, success of PCR validation of the 3' flank with the GoTaq mix using the L1 specific primer and the respective FS primer, success of Sanger sequencing of the 3' flank, success of amplifying the complete insertion with the Gotaq or Expand enzyme mix using the respective FS and ES primers, success of PCR validation of the 5' flank with the GoTaq mix using the L1nt112out and the respective ES primer, success of Sanger sequencing of the 5' flank, success of delineating the TSD, notes.

Colo1 sheet: ins. 2-41: high stringency data; ins. 45-PCM1: low stringency data; poly1-poly10: polymorphic germline insertions. Polymorphic germline insertions occurred frequently even in those samples, where few or no somatic insertions were detected, indicating that the low number of insertions in some tumors is not due to low

DNA quality, sample processing, or PCR validation failure. Colo2 sheet: ins. A1-E3: high stringency data. Only one insertion ("39") proved to be present also in normal tissue, representing a low false positive rate of tumor-specificity. We also recovered two insertions that were predicted to occur both in the normal and tumor tissues, but PCR analysis indicated that they were present exclusively in the tumor (ins. 21 and 35). Two insertions that could not be validated ("10" and "23") and first appeared to be tumor-specific turned out to be germline/colon-specific insertions after re-sequencing colo1/normal.

The 5 tumors that were sequenced by both L1-seq and RC-seq are tumor 1, 4, 6, 8, and 10. 11 high stringency L1Hs hits were found in these cancers by L1-seq, out of which 4 were detected by RC-seq as well (ins. 5, 9, 14, and 32). An L1 insertion in tumor 10 was detected by RC-seq, but was not present in the L1-seq data set (see Table S2).

Overall, the number of validated tumor-specific insertions is calculated in the following way: at the 3' junctions we PCR-validated 26/40 and 37/51 insertions from the colo1 and colo2 high stringency data sets, respectively. Out of 16 colo1 insertions represented by low stringency Illumina reads, we were able to validate 9. Thus, we PCR-validated the 3' flanks of 72 (26+37+9) of 107 (40+51+16) putative insertions. Altogether, out of 72 PCR-validated tumor-specific insertions, we could sequence either the 3' or the 5' junction in 69 cases (most cases were sequenced at the 3' junction). For 35 insertions, we successfully sequenced both junctions, thus we could determine TSDs and putatitve endonuclease sites.

Abbreviations: nw, not working (unsuccessful PCR validation attempt); N/A, data not available; TSD, target site duplication.

Table S4: Patient data.

Age indicates the time of surgical sample removal. The number of tumor-specific insertions reflects those that were successfully sequenced. Abbreviations: MSI, microsatellite instability; N/A, data not available.

Suppl. Text 1: Sanger sequencing results.

hg18 chromosomal coordinates are provided for validated L1-seq insertions.

REFERENCES

Asch, H. L., Eliacin, E., Fanning, T. G., Connolly, J. L., Bratthauer, G., and Asch, B. B. 1996. Comparative expression of the LINE-1 p40 protein in human breast carcinomas and normal breast tissues. *Oncol. Res.* **8:** 239-247.

Ashktorab, H., Smoot, D. T., Carethers, J. M., Rahmanian, M., Kittles, R., Vosganian, G., Doura, M., Nidhiry, E., Naab, T., Momen, B., et al. 2003. High incidence of microsatellite instability in colorectal cancer from African Americans. *Clin. Cancer Res.* **9:** 1112-1117.

Babushok, D. V., Ostertag, E. M., Courtney, C. E., Choi, J. M., and Kazazian, H. H.,Jr. 2006. L1 integration in a transgenic mouse model. *Genome Res.* **16:** 240-250.

Baillie, J. K., Barnett, M. W., Upton, K. R., Gerhardt, D. J., Richmond, T. A., De Sapio, F., Brennan, P. M., Rizzu, P., Smith, S., Fell, M., et al. 2011. Somatic retrotransposition alters the genetic landscape of the human brain. *Nature* **479:** 534-537.

Beck, C. R., Collier, P., Macfarlane, C., Malig, M., Kidd, J. M., Eichler, E. E., Badge, R. M., and Moran, J. V. 2010. LINE-1 retrotransposition activity in human genomes. *Cell* **141:** 1159-1170.

Beck, C. R., Garcia-Perez, J. L., Badge, R. M., and Moran, J. V. 2011. LINE-1 elements in structural variation and disease. *Annu. Rev. Genomics Hum. Genet.* **12:** 187-215.

Bogerd, H. P., Wiegand, H. L., Hulme, A. E., Garcia-Perez, J. L., O'Shea, K. S., Moran, J. V., and Cullen, B. R. 2006. Cellular inhibitors of long interspersed element 1 and Alu retrotransposition. *Proc. Natl. Acad. Sci. U. S. A.* **103:** 8780-8785.

Boissinot, S., Chevret, P., and Furano, A. V. 2000. L1 (LINE-1) retrotransposon evolution and amplification in recent human history. *Mol. Biol. Evol.* **17:** 915-928.

Bourc'his, D. and Bestor, T. H. 2004. Meiotic catastrophe and retrotransposon reactivation in male germ cells lacking Dnmt3L. *Nature* **431:** 96-99.

Bratthauer, G. L. and Fanning, T. G. 1992. Active LINE-1 retrotransposons in human testicular cancer. *Oncogene* **7:** 507-510.

Brouha, B., Schustak, J., Badge, R. M., Lutz-Prigge, S., Farley, A. H., Moran, J. V., and Kazazian, H. H.,Jr. 2003. Hot L1s account for the bulk of retrotransposition in the human population. *Proc. Natl. Acad. Sci. U. S. A.* **100:** 5280-5285.

Chen, H., Lilley, C. E., Yu, Q., Lee, D. V., Chou, J., Narvaiza, I., Landau, N. R., and Weitzman, M. D. 2006. APOBEC3A is a potent inhibitor of adeno-associated virus and retrotransposons. *Curr. Biol.* **16:** 480-485.

Cost, G. J., Feng, Q., Jacquier, A., and Boeke, J. D. 2002. Human L1 element target-primed reverse transcription in vitro. *EMBO J.* **21:** 5899-5910.

Coufal, N. G., Garcia-Perez, J. L., Peng, G. E., Marchetto, M. C., Muotri, A. R., Mu, Y., Carson, C. T., Macia, A., Moran, J. V., and Gage, F. H. 2011. Ataxia telangiectasia mutated (ATM) modulates long interspersed element-1 (L1) retrotransposition in human neural stem cells. *Proc. Natl. Acad. Sci. U. S. A.* **108:** 20382-20387.

de Koning, A. P., Gu, W., Castoe, T. A., Batzer, M. A., and Pollock, D. D. 2011. Repetitive elements may comprise over two-thirds of the human genome. *PLoS Genet.* **7:** e1002384.

Dewannieux, M., Esnault, C., and Heidmann, T. 2003. LINE-mediated retrotransposition of marked Alu sequences. *Nat. Genet.* **35:** 41-48.

Esnault, C., Maestre, J., and Heidmann, T. 2000. Human LINE retrotransposons generate processed pseudogenes. *Nat. Genet.* **24:** 363-367.

Ewing, A. D. and Kazazian, H. H.,Jr. 2011. Whole-genome resequencing allows detection of many rare LINE-1 insertion alleles in humans. *Genome Res.* **21:** 985-990.

Ewing, A. D. and Kazazian, H. H.,Jr. 2010. High-throughput sequencing reveals extensive variation in human-specific L1 content in individual human genomes. *Genome Res.* **20:** 1262-1270.

Feng, Q., Moran, J. V., Kazazian, H. H.,Jr, and Boeke, J. D. 1996. Human L1 retrotransposon encodes a conserved endonuclease required for retrotransposition. *Cell* **87:** 905-916.

Gasior, S. L., Wakeman, T. P., Xu, B., and Deininger, P. L. 2006. The human LINE-1 retrotransposon creates DNA double-strand breaks. *J. Mol. Biol.* **357:** 1383-1393.

Gilbert, N., Lutz, S., Morrish, T. A., and Moran, J. V. 2005. Multiple fates of L1 retrotransposition intermediates in cultured human cells. *Mol. Cell. Biol.* **25:** 7780-7795.

Goodier, J. L. and Kazazian, H. H.,Jr. 2008. Retrotransposons revisited: the restraint and rehabilitation of parasites. *Cell* **135:** 23-35.

Goodier, J. L., Ostertag, E. M., and Kazazian, H. H.,Jr. 2000. Transduction of 3'-flanking sequences is common in L1 retrotransposition. *Hum. Mol. Genet.* **9:** 653-657.

Hancks, D. C. and Kazazian, H. H. 2012. Active Human Retrotransposons: Variation and Disease. *Current Opinion in Genetics and Development* .

Hancks, D. C., Goodier, J. L., Mandal, P. K., Cheung, L. E., and Kazazian, H. H.,Jr. 2011. Retrotransposition of marked SVA elements by human L1s in cultured cells. *Hum. Mol. Genet.* **20:** 3386-3400.

Harris, C. R., Normart, R., Yang, Q., Stevenson, E., Haffty, B. G., Ganesan, S., Cordon-Cardo, C., Levine, A. J., and Tang, L. H. 2010. Association of nuclear localization of a long interspersed nuclear element-1 protein in breast tumors with poor prognostic outcomes. *Genes Cancer.* **1:** 115-124.

Holmes, S. E., Dombroski, B. A., Krebs, C. M., Boehm, C. D., and Kazazian, H. H.,Jr. 1994. A new retrotransposable human L1 element from the LRE2 locus on chromosome 1q produces a chimaeric insertion. *Nat. Genet.* **7:** 143-148.

Hormozdiari, F., Alkan, C., Ventura, M., Hajirasouliha, I., Malig, M., Hach, F., Yorukoglu, D., Dao, P., Bakhshi, M., Sahinalp, S. C., et al. 2011. Alu repeat discovery and characterization within human genomes. *Genome Res.* **21:** 840-849.

Hsu, F., Kent, W. J., Clawson, H., Kuhn, R. M., Diekhans, M., and Haussler, D. 2006. The UCSC Known Genes. *Bioinformatics* **22:** 1036-1046.

Huang, C. R., Schneider, A. M., Lu, Y., Niranjan, T., Shen, P., Robinson, M. A., Steranka, J. P., Valle, D., Civin, C. I., Wang, T., et al. 2010. Mobile interspersed repeats are major structural variants in the human genome. *Cell* **141:** 1171-1182.

Iskow, R. C., McCabe, M. T., Mills, R. E., Torene, S., Pittard, W. S., Neuwald, A. F., Van Meir, E. G., Vertino, P. M., and Devine, S. E. 2010. Natural mutagenesis of human genomes by endogenous retrotransposons. *Cell* **141:** 1253-1261.

Kaneko, H., Dridi, S., Tarallo, V., Gelfand, B. D., Fowler, B. J., Cho, W. G., Kleinman, M. E., Ponicsan, S. L., Hauswirth, W. W., Chiodo, V. A., et al. 2011. DICER1 deficit induces Alu RNA toxicity in age-related macular degeneration. *Nature* **471:** 325-330.

Kloor, M., Sutter, C., Wentzensen, N., Cremer, F. W., Buckowitz, A., Keller, M., von Knebel Doeberitz, M., and Gebert, J. 2004. A large MSH2 Alu insertion mutation causes HNPCC in a German kindred. *Hum. Genet.* **115:** 432-438.

Lee, E., Iskow, R., Yang, L., Gokcumen, O., Haseley, P., Luquette, L. J.,3rd, Lohr, J. G., Harris, C. C., Ding, L., Wilson, R. K., et al. 2012. Landscape of Somatic Retrotransposition in Human Cancers. *Science.*

Luan, D. D., Korman, M. H., Jakubczak, J. L., and Eickbush, T. H. 1993. Reverse transcription of R2Bm RNA is primed by a nick at the chromosomal target site: a mechanism for non-LTR retrotransposition. *Cell* **72:** 595-605.

Mathias, S. L., Scott, A. F., Kazazian, H. H.,Jr, Boeke, J. D., and Gabriel, A. 1991. Reverse transcriptase encoded by a human transposable element. *Science* **254:** 1808-1810.

Maxwell, P. H., Burhans, W. C., and Curcio, M. J. 2011. Retrotransposition is associated with genome instability during chronological aging. *Proc. Natl. Acad. Sci. U. S. A.* **108:** 20376-20381.

Miki, Y., Nishisho, I., Horii, A., Miyoshi, Y., Utsunomiya, J., Kinzler, K. W., Vogelstein, B., and Nakamura, Y. 1992. Disruption of the APC gene by a retrotransposal insertion of L1 sequence in a colon cancer. *Cancer Res.* **52:** 643-645.

Moran, J. V., DeBerardinis, R. J., and Kazazian, H. H.,Jr. 1999. Exon shuffling by L1 retrotransposition. *Science* **283:** 1530-1534.

Moran, J. V., Holmes, S. E., Naas, T. P., DeBerardinis, R. J., Boeke, J. D., and Kazazian, H. H.,Jr. 1996. High frequency retrotransposition in cultured mammalian cells. *Cell* **87:** 917-927.

Morrish, T. A., Gilbert, N., Myers, J. S., Vincent, B. J., Stamato, T. D., Taccioli, G. E., Batzer, M. A., and Moran, J. V. 2002. DNA repair mediated by endonuclease-independent LINE-1 retrotransposition. *Nat. Genet.* **31:** 159-165.

Muckenfuss, H., Hamdorf, M., Held, U., Perkovic, M., Lower, J., Cichutek, K., Flory, E., Schumann, G. G., and Munk, C. 2006. APOBEC3 proteins inhibit human LINE-1 retrotransposition. *J. Biol. Chem.* **281:** 22161-22172.

Muller, A., Edmonston, T. B., Dietmaier, W., Buttner, R., Fishel, R., and Ruschoff, J. 2004. MSI-testing in hereditary non-polyposis colorectal carcinoma (HNPCC). *Dis. Markers* **20:** 225-236.

Ohshima, K., Hattori, M., Yada, T., Gojobori, T., Sakaki, Y., and Okada, N. 2003. Whole-genome screening indicates a possible burst of formation of processed pseudogenes and Alu repeats by particular L1 subfamilies in ancestral primates. *Genome Biol*. **4:** R74.

Oricchio, E., Sciamanna, I., Beraldi, R., Tolstonog, G. V., Schumann, G. G., and Spadafora, C. 2007. Distinct roles for LINE-1 and HERV-K retroelements in cell proliferation, differentiation and tumor progression. *Oncogene* **26:** 4226-4233.

Ostertag, E. M., Goodier, J. L., Zhang, Y., and Kazazian, H. H.,Jr. 2003. SVA elements are nonautonomous retrotransposons that cause disease in humans. *Am. J. Hum. Genet.* **73:** 1444-1451.

Pavlicek, A., Paces, J., Zika, R., and Hejnar, J. 2002. Length distribution of long interspersed nucleotide elements (LINEs) and processed pseudogenes of human endogenous retroviruses: implications for retrotransposition and pseudogene detection. *Gene* **300:** 189-194.

Pickeral, O. K., Makalowski, W., Boguski, M. S., and Boeke, J. D. 2000. Frequent human genomic DNA transduction driven by LINE-1 retrotransposition. *Genome Res.* **10:** 411-415.

Raiz, J., Damert, A., Chira, S., Held, U., Klawitter, S., Hamdorf, M., Lower, J., Stratling, W. H., Lower, R., and Schumann, G. G. 2011. The non-autonomous retrotransposon SVA is trans-mobilized by the human LINE-1 protein machinery. *Nucleic Acids Res.* .

Refsland, E. W., Stenglein, M. D., Shindo, K., Albin, J. S., Brown, W. L., and Harris, R. S. 2010. Quantitative profiling of the full APOBEC3 mRNA repertoire in lymphocytes and tissues: implications for HIV-1 restriction. *Nucleic Acids Res.* **38:** 4274-4284.

Solyom, S., Ewing, A. D., Hancks, D. C., Takeshima, Y., Awano, H., Matsuo, M., and Kazazian, H. H.,Jr. 2012. Pathogenic orphan transduction created by a nonreference LINE-1 retrotransposon. *Hum. Mutat.* **33:** 369-371.

Stenglein, M. D. and Harris, R. S. 2006. APOBEC3B and APOBEC3F inhibit L1 retrotransposition by a DNA deamination-independent mechanism. *J. Biol. Chem.* **281:** 16837-16841.

Stewart, C., Kural, D., Stromberg, M. P., Walker, J. A., Konkel, M. K., Stutz, A. M., Urban, A. E., Grubert, F., Lam, H. Y., Lee, W. P., et al. 2011. A comprehensive map of mobile element insertion polymorphisms in humans. *PLoS Genet.* **7:** e1002236.

Su, L. K., Steinbach, G., Sawyer, J. C., Hindi, M., Ward, P. A., and Lynch, P. M. 2000. Genomic rearrangements of the APC tumor-suppressor gene in familial adenomatous polyposis. *Hum. Genet.* **106:** 101-107.

Su, Y., Davies, S., Davis, M., Lu, H., Giller, R., Krailo, M., Cai, Q., Robison, L., Shu, X. O., and Children's Oncology Group. 2007. Expression of LINE-1 p40 protein in pediatric malignant germ cell tumors and its association with clinicopathological parameters: a report from the Children's Oncology Group. *Cancer Lett.* **247:** 204-212.

Suzuki, J., Yamaguchi, K., Kajikawa, M., Ichiyanagi, K., Adachi, N., Koyama, H., Takeda, S., and Okada, N. 2009. Genetic evidence that the non-homologous end-joining repair pathway is involved in LINE retrotransposition. *PLoS Genet.* **5:** e1000461.

van der Klift, H. M., Tops, C. M., Hes, F. J., Devilee, P., and Wijnen, J. T. 2012. Insertion of an SVA element, a nonautonomous retrotransposon, in PMS2 intron 7 as a novel cause of lynch syndrome. *Hum. Mutat.* **33:** 1051-1055.

Wilhelm, C. S., Kelsey, K. T., Butler, R., Plaza, S., Gagne, L., Zens, M. S., Andrew, A. S., Morris, S., Nelson, H. H., Schned, A. R., et al. 2010. Implications of LINE1 methylation for bladder cancer risk in women. *Clin. Cancer Res.* **16:** 1682-1689.

Witherspoon, D. J., Xing, J., Zhang, Y., Watkins, W. S., Batzer, M. A., and Jorde, L. B. 2010. Mobile element scanning (ME-Scan) by targeted high-throughput sequencing. *BMC Genomics* **11:** 410.

Wood, L. D., Parsons, D. W., Jones, S., Lin, J., Sjoblom, T., Leary, R. J., Shen, D., Boca, S. M., Barber, T., Ptak, J., et al. 2007. The genomic landscapes of human breast and colorectal cancers. *Science* **318:** 1108-1113.

Yang, N., Zhang, L., Zhang, Y., and Kazazian, H. H.,Jr. 2003. An important role for RUNX3 in human L1 transcription and retrotransposition. *Nucleic Acids Res.* **31:** 4929-4940.

Yoder, J. A., Walsh, C. P., and Bestor, T. H. 1997. Cytosine methylation and the ecology of intragenomic parasites. *Trends Genet.* **13:** 335-340.

INSERTION	TUMOR	CHR.	CHR. LOCATION (hg18)	CHR. LOCATION (hg19)	L1 5' junction	Inferred L1 size (bp)	IDENTITY TO L1RP (%)	poly(A) LENGTH (bp)	TSD	Endo site	NOTES
Ins. 5	1	10	56731539-56731701	57061533-57061695	5898-5934	122	100	73	AACAGAAGTCTCA (13 bp)	TGTT/GA	5' junction with RC-seq
Ins. 6	15	11	20389184-20389665	20432608-20433089	5779-5432	588	100	17	AAATACTTTTAGTT (14 bp)	ATTT/TA	partly inverted L1
					5780-5965		99				
Ins. 7	1	11	36145260-36145460	36188684-36188884	5786-5893	234	100	16-70	GAAGAAATATC (11bp)	CTTC/AG	
Ins. 9	1	11	114813023-114813333	115307813-115308123	5161-5849	859	100	71	A (1bp)	T/AA	3' junction also with RC-seq
Ins. 24	10	3	1873003-1873267	1898003-1898267	5473-6019	547	99	32-37	AGAATTTA (8bp)	TTCT/AA	
Ins. 30	15	3	175764832-175764906	174282138-174282212	5762-6019	258	99	42-43	none	TTTC/AG	potentially endo independent
Ins. 32	1	4	166273011-166273097	166053561-166053647	5399-6019	621	100	39	none	TTAT/CA	3' junction also with RC-seq
Ins. 35	1	5	165976534-165976920	166043956-166044342	5640-6019	380	100	23-104	none, 6 bp deletion	GTTT/TT	potentially endo independent
Ins. 36	6	6	91768021-91768340	91711300-91711619	5818-6018/6019	202	99	26-28	(T)AGTTGGTAGCTTTTT (15/16 bp)	AACT/AA	inverted poly(A) inserted in front of L1 nt. 5818; untemplated nt.-s AAAGCCTG in between
Ins. 47	15	11	90728127-90728299	91088479-91088651	5693-5894	327	100	74	none	ACAT/TG	potentially endo independent
Ins. 50	10	16	63628221-63628561	65070720-65071060	5245-5172	775	100	21+18-29 (3' transduction)	AAGAAGCTA (9 bp)	TCTT/AG	insertion into *CDH11* ; L1 inversion; 124 bp 3' transduction from chr. 1
Ins. 57	4	7	54612665-54612869	54645171-54645375	5308-4921	1077	100	83	AAGAATACCATAGGTTGG (18 bp)	TCTT/AT	partly inverted L1 with L1 deletion
					5331-5628		99				
Ins. A2	6645	1	118179594-118179855	118378071-118378332	5626-5916	394	99	45	AAAAAATTACAACTACA (17 bp)	TTTT/AC	untemplated TGC nt.-s at 5' breakpoint
Ins. A4	1775	1	186265021-186265327	187998398-187998704	5118-5800	902	99	17	none	ATAT/TG	potentially endo
Ins. A5	1775	10	52852490-52852780	53182484-53182774	5560-5890	460	N/A	15	AAAAAACAAAAAA (13 bp)	TTTT/AA	untemplated AA nt.-s at 5' breakpoint
Ins. A8	17	12	18980506-18980824	19089239-19089557	5498-6019	522	99	46	AAAAAAG (7 bp)	TTTT/AT	
Ins. B2	1552	17	13914476-13914781	13973751-13974056	5832-6019	188	100	25-34	GAAATT (6 bp)	TTTC/AT	
Ins. B4	1775	18	67449071-67449391	69298091-69298411	5525-5885	495	100	21	AAAAGTCC (8 bp)	AAGT/AC	
Ins. B5	17	2	140975700-140975940	141259230-141259470	5695-5907	325	100	35	AAAAGTAGCAAAT (13 bp)	TTTT/GA	
Ins. B6	1775	2	188158976-188159118	188450731-188450873	4909-5371	1111	N/A	11	AAAAATGCATAA (12 bp)	TTTT/AT	
Ins. B7	1775	2	188578469-188578710	188870224-188870465	5570-5907	450	100	31	TAAAAGATCTTAAATA (16 bp)	TTTA/AA	
Ins. B9	1552	3	141880688-141880901	140397998-140398211	3161-2454	2218	99	27	AAAAGTTACAGGTATT (16 bp)	TTTT/AA	partly inverted L1 with L1 deletion
					4510-4608		100				
Ins. B10	1775	4	93068869-93069099	92849846-92850076	5896-6019	124	99	36-40	AAAG (4 bp)	CTTT/AC	
Ins. C4	6645	5	62265644-62265857	62229888-62230101	5270-5750	750	99	26	none	TTTA/TG	potentially endo independent
Ins. C6	1775	6	87790188-87790349	87733469-87733630	5807-5903	213	100	16	AAGAGATTGGCAAATGA (17 bp)	TCTT/AT	
Ins. C7	1775	6	132427126-132427288	132385433-132385595	5703-5319	384	100	28	AAAAGAAATATGTC (14 bp)	TTTT/AG	partly inverted L1 with L1 deletion
					5721-5891		100				
Ins. C8	1775	7	43206340-43206484	43239815-43239959	5892-6019	128	98	27-50	none, 1 bp deletion	CGTC/AT	potentially endo independent
Ins. C10	6645	7	71370938-71371265	71733002-71733329	5830-6019	190	100	48-49	A (1 bp)	T/AA	
Ins. D5	1775	8	111653589-111653790	111584413-111584614	4861-4525	1435	100	40	A (1 bp)	T/CA	partly inverted L1 with L1 deletion
					4922-5269		99				
Ins. D7	1775	8	140519447-140519608	140450265 140450426	5214-5867	806	N/A	30	AAAAAAGGACT (11 bp)	TTTT/AT	
ins. D9	17	X	18694952-18695143	18785031-18785222	4854-5680	1166	99	46	ATAAAAATGAG (11 bp)	TTAT/AG	
Ins. D10	1775	X	83860994-83861183	83974338-83974527	4504-4011	1516	N/A	76	TAAAACAGAGAACA (14 bp)	TTTA/AT	partly inverted L1
Ins. D11	1775	X	87182336-87182515	87295680-87295859	5913-6019	107	100	21-26	none, 1 bp deletion	CTTT/AT	
Ins. D12	2853	X	108163640-108163825	108276984-108277169	5399-5361	510	100	59	AAAAGTTAAGTTGTT (15 bp)	TTTT/AT	partly inverted L1 with L1 deletion;
					5549-5908		100				
Ins. E1	1775	X	108585628-108585763	108698972-108699107	5655-5644	363	100	13	AAAAATCAACATACCCA (17 bp)	TTTT/AA	partly inverted L1 with L1 deletion
					5669-5890		99				

Table 1

Figure 1

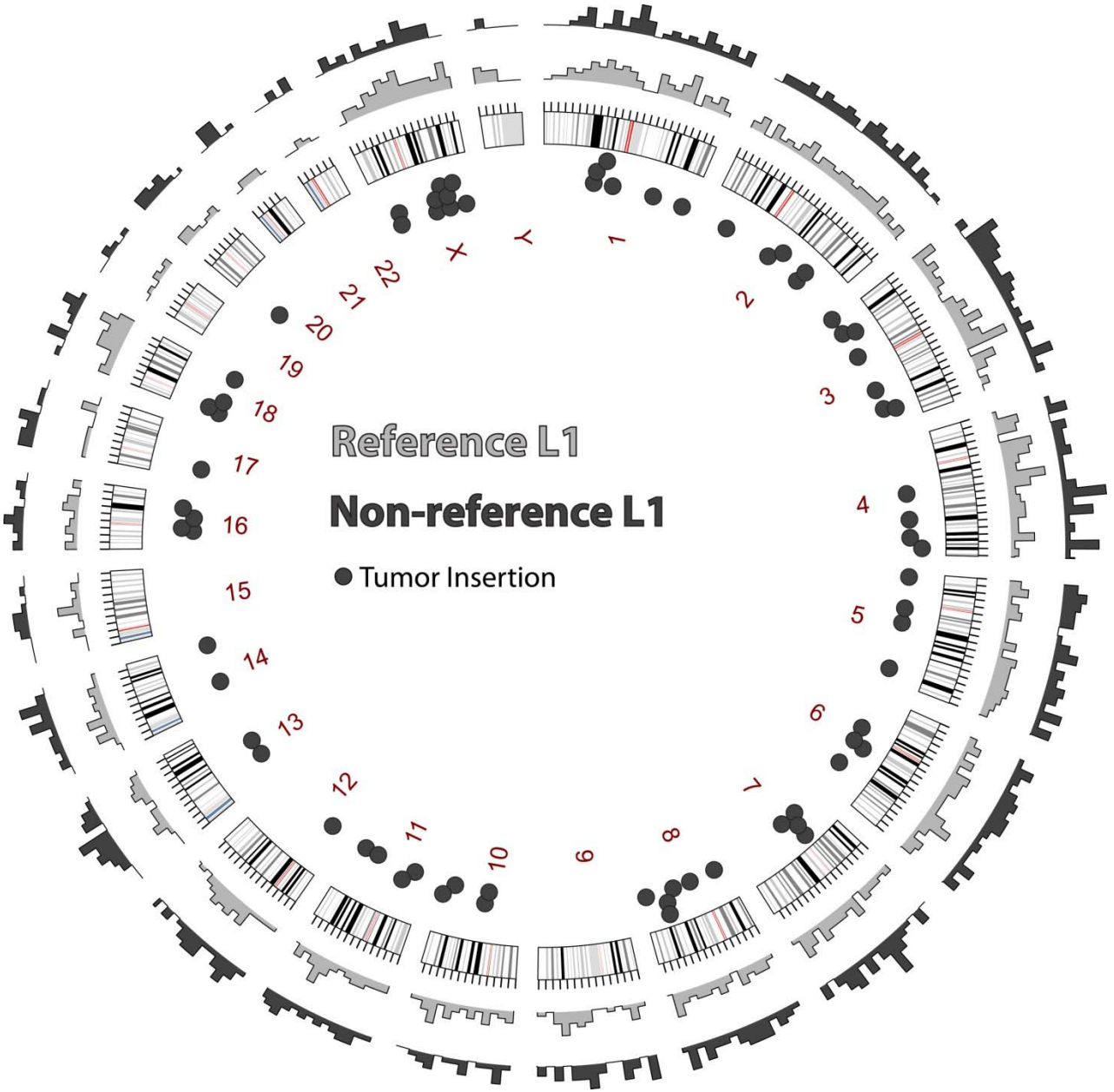

Figure 2A

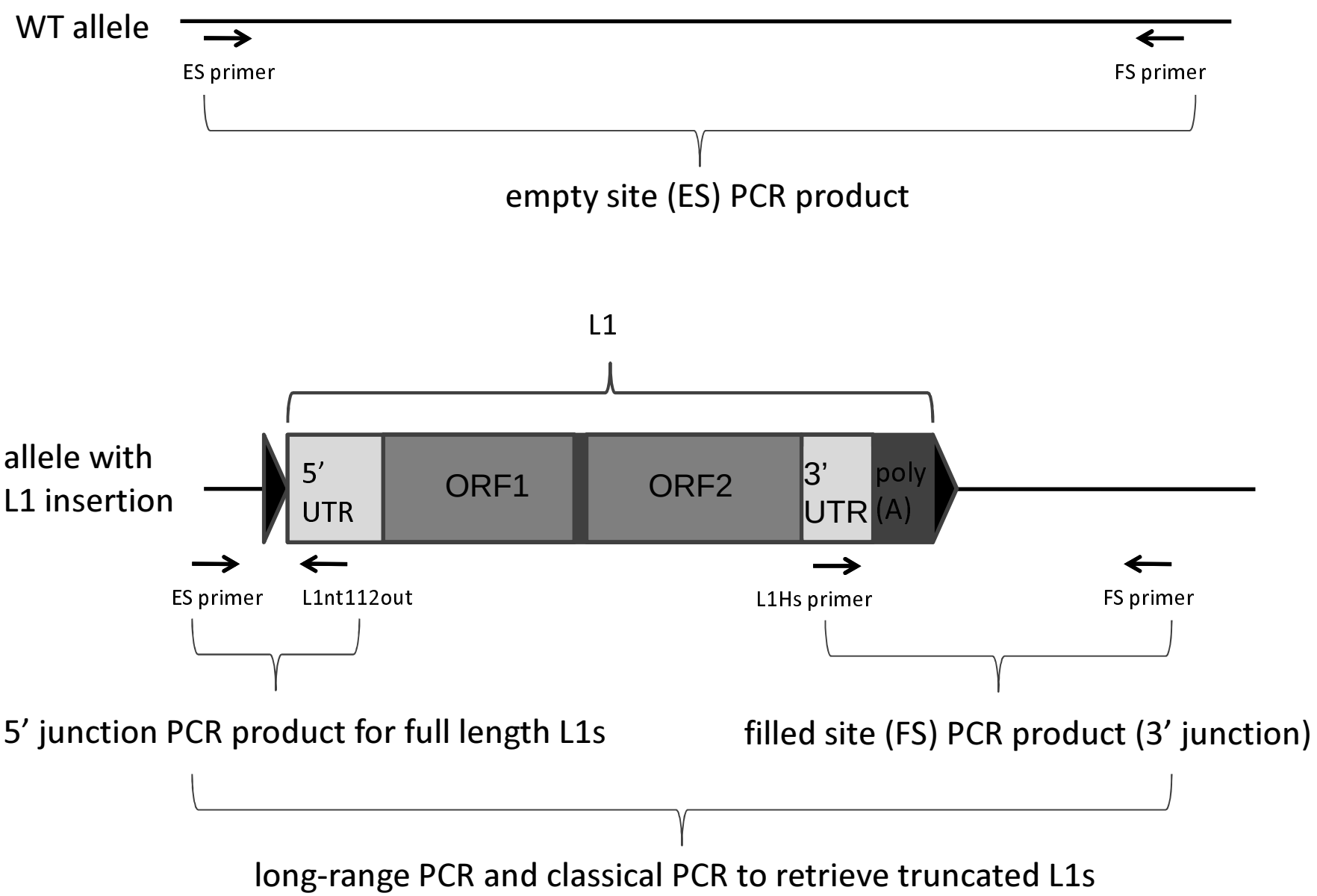

Figure 2B

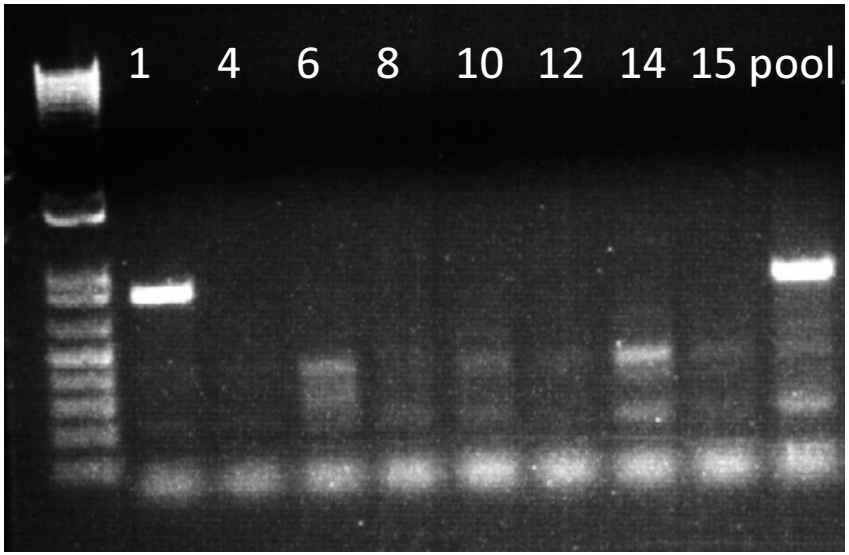

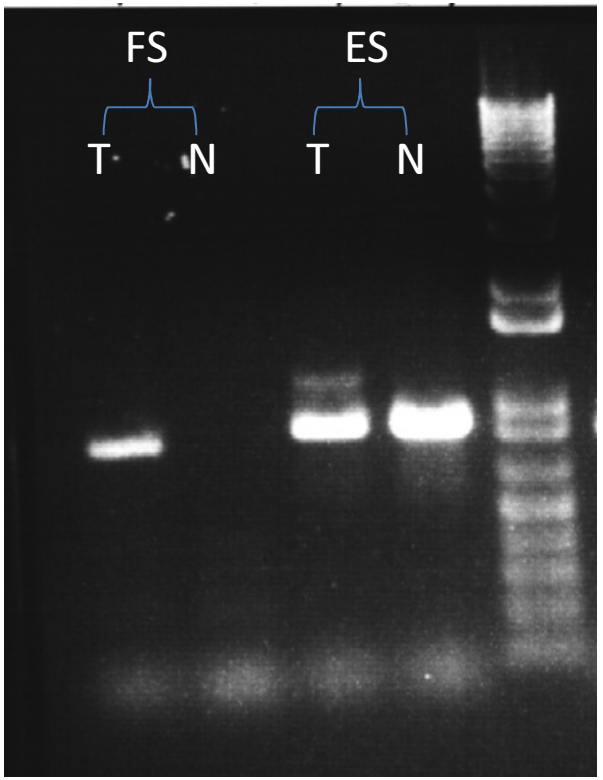

Figure 3

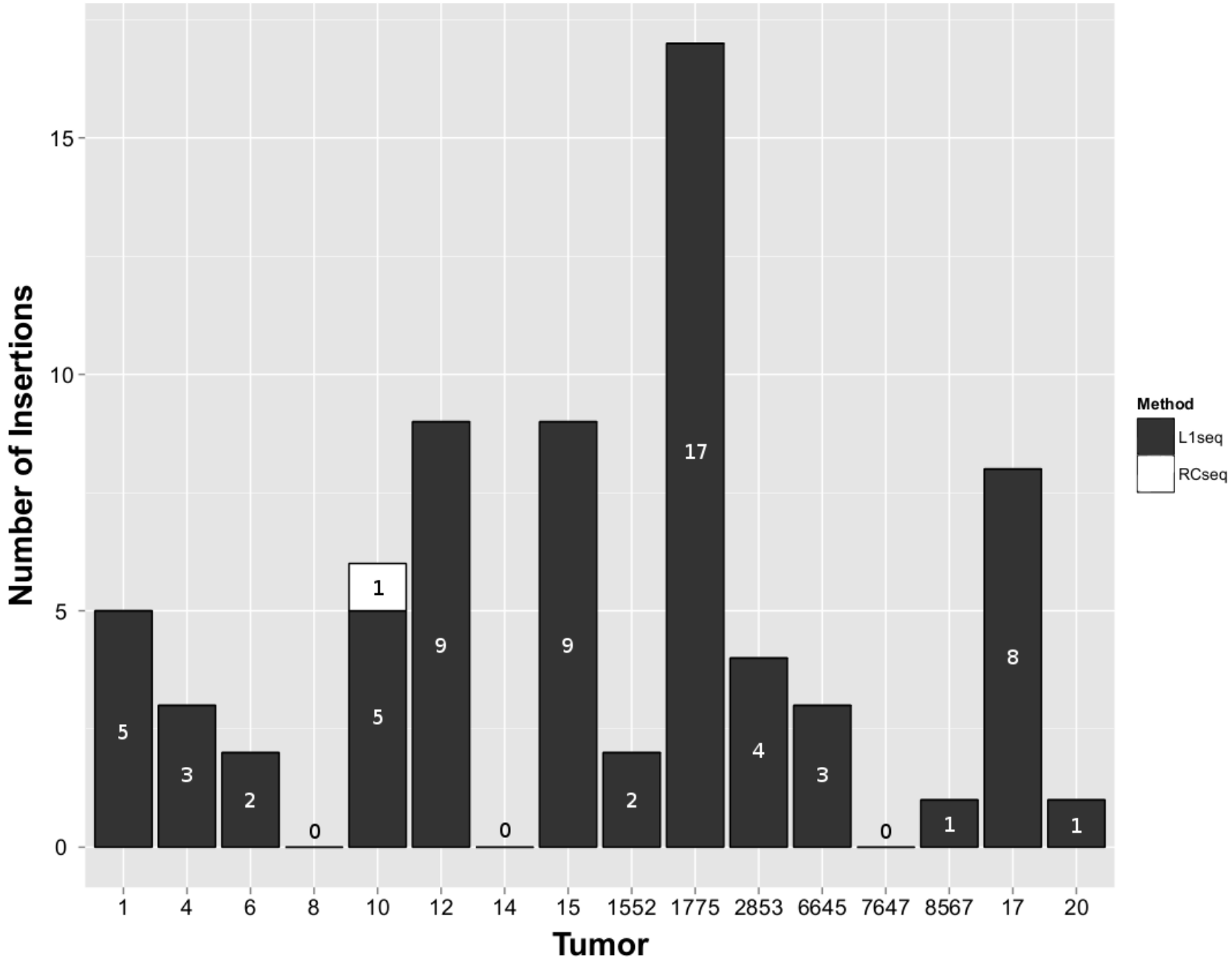

Figure 4